

# PROPOSAL

for

ENIGMA-PGC PTSD

## Dynamic Resting-State Functional Connectivity in Posttraumatic Stress Disorder

Delin Sun Ph.D.<sup>a,b</sup>  
Rajendra A. Morey, M.D.<sup>a,b,c</sup>

<sup>a</sup> Duke-UNC Brain Imaging and Analysis Center, Duke University

<sup>b</sup> Department of Veteran Affairs (VA) Mid-Atlantic Mental Illness Research, Education and Clinical Center

<sup>c</sup> Department of Psychiatry and Behavioral Sciences, Duke University

Delin Sun, Ph.D.  
3022 Croasdaile Dr, Room 310  
Durham, NC 27705 USA  
Phone: 919-638-4348  
E-mail: delin.sun@duke.edu

Rajendra A. Morey, M.D.  
40 Duke Medicine Circle, Room 414  
Durham, NC 27710 USA  
Phone: 919-286-0411 ext. 6425  
Facsimile: 919-416-5912  
E-mail: rajendra.morey@duke.edu

**Abstract (<150 words)**

Posttraumatic stress disorder (PTSD) is associated with abnormal static resting-state functional connectivity (rsFC), especially in amygdala, hippocampus, anterior cingulate cortex (ACC) and medial prefrontal cortex (mPFC). However, little is known about PTSD-related dynamic changes in functional connectivity. We hypothesize that patients with PTSD is associated with reduced temporal variability of functional connectivity than trauma-exposed controls based on compromised abilities of PTSD patients to dynamically adjust behaviors and thoughts to changing conditions and a preoccupation with trauma-related experiences. We will compare patients with PTSD (N~1500) to trauma-exposed controls (N~1500) from ENIGMA-PGC PTSD project on dynamic rsFC based on the standard deviations in rsFC of amygdala, hippocampus and mPFC over a series of sliding windows. The proposed research may advance knowledges of fluctuating communications among brain systems in PTSD.

Keywords: Dynamic Functional Connectivity; Resting-State fMRI; PTSD; amygdala; hippocampus; mPFC.

## **Background:**

Posttraumatic Stress Disorder (PTSD) is a mental health problem that some people develop after experiencing or witnessing a life-threatening event, like combat, a natural disaster, a car accident, or sexual assault (Shalev *et al*, 2017). Previous studies have documented several PTSD-related brain areas including amygdala, hippocampus, medial prefrontal cortex (mPFC), anterior cingulate cortex (ACC) and insula (Brown *et al*, 2014; Morey *et al*, 2012; Morey *et al*, 2016), that are associated with emotion, memory and executive functions (Shalev *et al*, 2017). The methodological development in resting-state functional magnetic resonance imaging (fMRI) method makes it straightforward to compare brain activity across groups without relying on task demands and instructions, whereas functional connectivity is a common analysis for resting-state fMRI data and refers to measures of correlation between pairs of fMRI time series obtained from different brain regions (Lee *et al*, 2013; van den Heuvel and Pol, 2010). Previous studies showed that PTSD is associated with larger resting-state functional connectivity (rsFC) between amygdala and insula (Rabinak *et al*, 2011), smaller amygdala-hippocampus rsFC (Sripada *et al*, 2012), and larger amygdala-ACC/dorsal mPFC rsFC (Brown *et al*, 2014). A recent review reported increased rsFC in salience network but decreased rsFC in default mode network in PTSD (Koch *et al*, 2016).

Most of rsFC studies on PTSD utilized the static functional connectivity method, which assumes that functional connectivity between regions is stationary over time (Koch *et al*, 2016). However, static rsFC outputs only one connectivity value per voxel during the entire length of the scan, and potentially leads to loss of information and sensitivity to the underlying dynamic neural processes (Allen *et al*, 2014). By contrast, nonstationary and spontaneous relationships exist in rsFC regardless of conscious cognitive processing (Hutchison *et al*, 2013). Further, dynamic variations in rsFC are relevant to changes in vigilance (Thompson *et al*, 2013), arousal (Chang *et al*, 2013), emotional state (Cribben *et al*, 2012), and behavioral performance (Jia *et al*, 2014). A recent study by Jin *et al* (2017) showed that patients with PTSD were associated with stronger static but weaker dynamic rsFC, suggesting compromised abilities in PTSD patients to dynamically adjust behaviors and thoughts to changing conditions. The decreased dynamic rsFC has also been detected in other psychiatric disorders (Sakoglu *et al*, 2010), and was found to relate with compromised behavioral performance in healthy controls (Jia *et al*, 2014). Interestingly, dynamic rsFC exhibited higher accuracy than static rsFC in differentiating PTSD from trauma-exposed controls with machine learning (Jin *et al*, 2017).

Unfortunately, to the best of our knowledge, there is only one study by Jin *et al* (2017) investigating dynamic rsFC in patients with PTSD among Chinese earthquake survivors. The sample size in their study is also relatively small ( $N < 100$  per group). Little is known about whether their findings could be generalized to a larger sample size with participants of diverse trauma types. Moreover, it is still unclear how rsFC is affected between areas important to PTSD, including amygdala, hippocampus, ACC and mPFC. By expanding our investigation into a larger sample size ( $N \sim 1,500$  per group) with participants from diverse sites and accompanied with different trauma types, we may delineate the dynamic functional connections between areas in PTSD without the bias of trauma type and demographic information. The knowledge gained may contribute to advancing our understanding of the neurobiology of PTSD and in future may shed light on treatments for PTSD.

## **Specific Aims and Objectives:**

**Aim:** Investigate Dynamic rsFC in PTSD. Diagnosis of PTSD will be performed with the Clinician Administration PTSD Scale (CAPS). Measures of brain activity from resting-state functional MRI scans, obtained from the ENIGMA-PTSD project proposed in this application, will be analyzed for dynamic rsFC. Given the compromised abilities of PTSD patients to dynamically

adjust behaviors and thoughts to changing conditions and a preoccupation with trauma-related experiences, we hypothesize that PTSD patients compared to trauma-exposed controls will be associated with reduced dynamic rsFC between important seed areas, including amygdala, hippocampus, ACC and mPFC, and the rest of the brain.

### Research Plan:

Participants: We will target PTSD patients from the ENIGMA-PTSD project to achieve detailed clinical measures including PTSD scores. The sample size of  $N \sim 1500$  per group will provide excellent power to make inferences about brain dynamic rsFC associated with differences between PTSD patients and trauma-exposed controls. We will exclude all participants with Axis I disorders except those with PTSD, major depression, and past substance abuse. We will exclude participants with significant neurological disorders (e.g. seizure, stroke), major neurological surgery, TBI, and significant cardiorespiratory compromise (e.g. COPD). However, present substance abuse of nicotine products will be permitted. All participants with contraindication to obtaining MRI scanning or those with claustrophobia will be excluded.

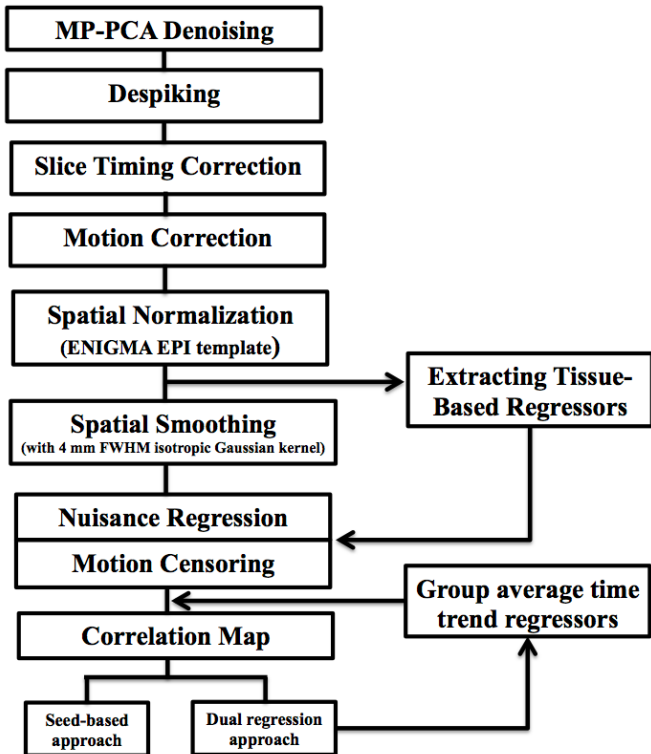


Figure 1. Flowchart of ENIGMA rsfMRI analysis pipeline (adapted from Adhikari *et al* (2018)).

Preprocessing: Following the ENIGMA analysis pipeline for resting-state fMRI data implemented in the AFNI software (Fig. 1) (Adhikari *et al*, 2018), we will first apply Marchenko-Pastur distribution-based principal components analysis (MP-PCA) for denoising (Veraart *et al*, 2016), to improve signal-to noise ratio (SNR) and temporal SNR (tSNR) properties of the time series data, with no loss of spatial resolution of the image and without the introduction of additional partial volume effects. We will then correct spatial distortions associated with long-TE gradient echo imaging using the gradient-echo 'fieldmap' or the reversed-gradient

approach. After that, we will correct the time of acquisition of each slice. Next, we will correct head motion by registering each functional volume to the volume with the minimum outlier fraction, where each transformation is concatenated with the transformation to standard space, to avoid unnecessary interpolation. We will further spatially normalize images to the ENIGMA EPI template in Montreal Neurological Institute (MNI) standard space for group analysis, and then smooth the images with a 4-mm kernel. We will then regress out the effects of nuisance variables such as the linear trend, 6 motion parameters (3 rotational and 3 translational directions), their 6 temporal derivatives (rate of change in rotational and translational motion) and time courses from the local white matter and cerebrospinal fluid (CSF) from lateral ventricles. Finally, we will censor the time points with excessive motion ( $> 0.2$  mm) estimated as the magnitude of displacement from one time point to the next, including neighboring time points and outlier voxels fraction ( $> 0.1$ ) were censored from statistical analysis. We will make outlier

images based on the time points with excessive motion, and enter then into the individual-level general linear model to remove the influence of these time points on estimates of functional connectivity while maintaining the temporal structure of the data.

**Individual-level Analyses:** Voxel-wise seed-based functional connectivity analyses will be performed using the CONN toolbox (Whitfield-Gabrieli *et al*, 2012) and in-house scripts written in Matlab (version R2016b). The seed regions of interest will be amygdala, hippocampus, ACC and mPFC that are defined by the anatomical mask images from the WFU\_PickAtlas software (<http://fmri.wfubmc.edu/software/pickatlas>). Following Kaiser *et al* (2016), the time course will be segmented into 36-s windows, sliding the onset of each window by 18 s, for a total of 15–19 windows (depending on length of the functional scan). The duration of sliding windows is selected to optimize the balance between capturing rapidly shifting dynamic relationships (with shorter windows) and achieving reliable estimates of the correlated activity between regions (Leonardi and Van De Ville, 2015). Next, the Fisher's z-transformed Pearson's correlation coefficient will be computed for each sliding window between the truncated time course of the seed and that of all other voxels, yielding a set of sliding-window beta maps for each participant. Dynamic rsFC will be estimated by calculating the SD in beta values at each voxel.

**Group-level analyses:** For each seed area, individual dynamic rsFC maps will be entered into a whole-brain t-test to investigate the between-group differences. Correlation analyses to examine the relationship between severity of PTSD and dynamic rsFC will be conducted within the PTSD group based on a correlation between CAPS scores and dynamic rsFC at each voxel per seed region. Age, sex, depression severity, traumatic brain injury (TBI), alcohol use, childhood trauma exposure, adult trauma exposure, medication status and scanner site will be included as covariates of no interest. Group-level effects will be considered significant if results are height-thresholded at  $p < 0.001$  and survive  $p < 0.05$  cluster-level false discovery rate (FDR) corrections. In the aforementioned mega-analysis, we will pool all subjects together to calculate the functional connections between seed areas and the rest of the brain, and will find some target areas significantly connected with seeds. The mega-analysis will include a covariate for site. Sites with multiple scanners will be subdivided into multiple sites. To avoid being biased by the mega-analysis due stratification or interaction effects, we will then extract the values of functional connections between seeds and targets, and enter them into a meta-regression approach to validate the findings. We will also explore available whole brain meta-regression analytic strategies.

**References:**

Adhikari BM, Jahanshad N, Shukla D, Glahn DC, Blangero J, Reynolds RC, *et al* (2018). Heritability estimates on resting state fMRI data using ENIGMA analysis pipeline. *Pac Symp Biocomput* **23**: 307-318.

Allen EA, Damaraju E, Plis SM, Erhardt EB, Eichele T, Calhoun VD (2014). Tracking Whole-Brain Connectivity Dynamics in the Resting State. *Cereb Cortex* **24**(3): 663-676.

Brown VM, Labar KS, Haswell CC, Gold AL, McCarthy G, Morey RA, *et al* (2014). Altered Resting-State Functional Connectivity of Basolateral and Centromedial Amygdala Complexes in Posttraumatic Stress Disorder. *Neuropsychopharmacol* **39**(2): 351-359.

Chang C, Metzger CD, Glover GH, Duyn JH, Heinze HJ, Walter M (2013). Association between heart rate variability and fluctuations in resting-state functional connectivity. *Neuroimage* **68**: 93-104.

Cribben I, Haraldsdottir R, Atlas LY, Wager TD, Lindquist MA (2012). Dynamic connectivity regression: Determining state-related changes in brain connectivity. *Neuroimage* **61**(4): 907-920.

Hutchison RM, Womelsdorf T, Allen EA, Bandettini PA, Calhoun VD, Corbetta M, *et al* (2013). Dynamic functional connectivity: promise, issues, and interpretations. *Neuroimage* **80**: 360-378.

Jia H, Hu X, Deshpande G (2014). Behavioral relevance of the dynamics of the functional brain connectome. *Brain Connect* **4**(9): 741-759.

Jin CF, Jia H, Lanka P, Rangaprakash D, Li LJ, Liu TM, *et al* (2017). Dynamic Brain Connectivity Is a Better Predictor of PTSD than Static Connectivity. *Hum Brain Mapp* **38**(9): 4479-4496.

Kaiser RH, Whitfield-Gabrieli S, Dillon DG, Goer F, Beltzer M, Minkel J, *et al* (2016). Dynamic Resting-State Functional Connectivity in Major Depression. *Neuropsychopharmacol* **41**(7): 1822-1830.

Koch SBJ, van Zuiden M, Nawijn L, Frijling JL, Veltman DJ, Olff M (2016). Aberrant Resting-State Brain Activity in Posttraumatic Stress Disorder: A Meta-Analysis and Systematic Review. *Depress Anxiety* **33**(7): 592-605.

Lee MH, Smyser CD, Shimony JS (2013). Resting-State fMRI: A Review of Methods and Clinical Applications. *Am J Neuroradiol* **34**(10): 1866-1872.

Leonardi N, Van De Ville D (2015). On spurious and real fluctuations of dynamic functional connectivity during rest. *Neuroimage* **104**: 430-436.

Morey RA, Gold AL, LaBar KS, Beall SK, Brown VM, Haswell CC, *et al* (2012). Amygdala volume changes in posttraumatic stress disorder in a large case-controlled veterans group. *Archives of general psychiatry* **69**(11): 1169-1178.

Morey RA, Haswell CC, Hooper SR, De Bellis MD (2016). Amygdala, Hippocampus, and Ventral Medial Prefrontal Cortex Volumes Differ in Maltreated Youth with and without Chronic Posttraumatic Stress Disorder. *Neuropsychopharmacol* **41**(3): 791-801.

Rabinak CA, Angstadt M, Welsh RC, Kenndy AE, Lyubkin M, Martis B, *et al* (2011). Altered amygdala resting-state functional connectivity in post-traumatic stress disorder. *Front Psychiatry* **2**: 62.

Sakoglu U, Pearson GD, Kiehl KA, Wang YM, Michael AM, Calhoun VD (2010). A method for evaluating dynamic functional network connectivity and task-modulation: application to schizophrenia. *Magn Reson Mater Phy* **23**(5-6): 351-366.

Shalev A, Liberzon I, Marmar C (2017). Post-Traumatic Stress Disorder. *New Engl J Med* **376**(25): 2459-2469.

Sripada RK, King AP, Garfinkel SN, Wang X, Sripada CS, Welsh RC, *et al* (2012). Altered resting-state amygdala functional connectivity in men with posttraumatic stress disorder. *J Psychiatr Neurosci* **37**(4): 241-249.

Thompson GJ, Magnuson ME, Merritt MD, Schwab H, Pan WJ, McKinley A, *et al* (2013). Short-Time Windows of Correlation Between Large-Scale Functional Brain Networks Predict Vigilance Intraindividually and Interindividually. *Hum Brain Mapp* **34**(12): 3280-3298.

van den Heuvel MP, Pol HEH (2010). Exploring the brain network: A review on resting-state fMRI functional connectivity. *Eur Neuropsychopharm* **20**(8): 519-534.

Veraart J, Novikov DS, Christiaens D, Ades-Aron B, Sijbers J, Fieremans E (2016). Denoising of diffusion MRI using random matrix theory. *Neuroimage* **142**: 394-406.

Whitfield-Gabrieli S, Nieto-Castanon A (2012). Conn: a functional connectivity toolbox for correlated and anticorrelated brain networks. *Brain Connect* **2**(3): 125-141.